

Interface photoluminescence in type II broken-gap $P\text{-Ga}_{0.84}\text{In}_{0.16}\text{As}_{0.22}\text{Sb}_{0.78}/p\text{-InAs}$ single heterostructures

K. D. Moiseev,^{a)} A. Krier,^{b)} and Yu. P. Yakovlev^{c)}

Department of Physics, Lancaster University, Lancaster LA1 4YB, United Kingdom

(Received 19 June 2001; accepted for publication 18 July 2001)

Mid-infrared photoluminescence has been observed from interface transitions in high quality, abrupt $P\text{-Ga}_{0.84}\text{In}_{0.16}\text{As}_{0.22}\text{Sb}_{0.78}/p\text{-InAs}$ heterojunctions grown by liquid phase epitaxy from an In-rich melt. The $\text{Ga}_{0.84}\text{In}_{0.16}\text{As}_{0.22}\text{Sb}_{0.78}$ quaternary epitaxial layer was unintentionally doped and grown lattice matched on to a (100) oriented p -type InAs substrate, resulting in a $P\text{-}p$ isotype heterojunction. The photoluminescence emission spectra were investigated and exhibited three pronounced emission bands in the spectral region from 0.30 to 0.68 eV; $h\nu_1=0.317$ eV, $h\nu_2=0.380$ eV, and $h\nu_L=0.622$ eV. The emission band $h\nu_1$ was identified with radiative transitions between electron and hole quantum well subbands in the semimetal channel at the $P\text{-GaIn}_{0.03}\text{As}_{0.10}\text{Sb}/p\text{-InAs}$ interface, while the $h\nu_2$ band originates from radiative transitions involving deep acceptor states in the InAs substrate. The high-energy recombination $h\nu_L$ is characteristic of the $\text{Ga}_{0.84}\text{In}_{0.16}\text{As}_{0.22}\text{Sb}_{0.78}$ bulk quaternary layer. © 2001 American Institute of Physics. [DOI: 10.1063/1.1402968]

INTRODUCTION

There is a growing interest in semiconductor lasers emitting in the mid-infrared spectral region ($3\text{--}5\text{ }\mu\text{m}$) since these lasers can be used in the trace gas detection of a variety of species which have characteristic absorption fingerprints in this range, leading to applications such as remote sensing, molecular spectroscopy, and ecological monitoring. Other potential applications include, infrared countermeasures and free space optical communications within the ($3\text{--}5\text{ }\mu\text{m}$) atmospheric transmission window. However, it is necessary not only to achieve the target wavelength, but also to obtain operation at room temperature before these devices can become widely used in practice. The quaternary solid solutions $\text{Ga}_{1-x}\text{In}_x\text{As}_y\text{Sb}_{1-y}$ and their heterojunctions formed with InAs are promising materials systems for the fabrication of efficient optoelectronic devices operating in this spectral range.^{1,2} The unique type-II band alignment of the broken-gap $\text{Ga}_{1-x}\text{In}_x\text{As}_y\text{Sb}_{1-y}/\text{InAs}$ heterojunction offers the possibility of a substantial reduction in Auger recombination which is thought to be the main loss mechanism in narrow-gap III-V lasers designed for room temperature operation. Adjusting the In content in the quaternary layer enables control of both the energy gap of the solid solution and the band offsets at the interface. Due to the nature of the crossed band line up the wide-gap $\text{Ga}_{1-x}\text{In}_x\text{As}_y\text{Sb}_{1-y}$ alloy-InAs system in the composition range $x<0.22$, electrons and holes are spatially separated and localized in self-consistent quantum wells on the InAs and $\text{Ga}_{1-x}\text{In}_x\text{As}_y\text{Sb}_{1-y}$ sides of the heterointerface, respectively.³ This separation should result in Auger suppression, which can lead to improvement of laser

temperature characteristics, while the combination of wide gap alloy and narrow gap InAs means that intervalence band resonances are also avoided.⁴ Recently, tunnel-injection diode lasers based on type II recombination across the broken-gap $\text{Ga}_{1-x}\text{In}_x\text{As}_y\text{Sb}_{1-y}/\text{InAs}$ heterojunction exhibited a good performance at low temperatures but laser emission was limited to 196 K in the pulsed regime.⁵

In order to fabricate an effective heterointerface diode laser it is necessary to obtain information about the associated radiative transitions and their quantum efficiency. So far, only the photoluminescence of bulk $\text{Ga}_{1-x}\text{In}_x\text{As}_y\text{Sb}_{1-y}$ solid solutions in the composition range $0.08<x<0.22$ has been studied over the temperature range $T=4\text{--}80\text{ K}$ ^{6,7} and (tunnel-assisted) interface electroluminescence in type II single $p\text{-Ga}_{0.84}\text{In}_{0.16}\text{As}_{0.22}\text{Sb}_{0.78}/p\text{-InAs}$ heterostructures has also been observed at 77 K.⁸ In this article we report the observation of interface-induced photoluminescence in type II broken-gap $p\text{-Ga}_{0.84}\text{In}_{0.16}\text{As}_{0.22}\text{Sb}_{0.78}/p\text{-InAs}$ heterostructures.

EXPERIMENTAL PROCEDURES

The GaSb-rich $\text{Ga}_{0.84}\text{In}_{0.16}\text{As}_{0.22}\text{Sb}_{0.78}$ quaternary solid solution was grown lattice matched on (100) oriented Zn-doped InAs (P -type) substrates by liquid phase epitaxy (LPE). The growth was performed in a conventional horizontal graphite slider boat under purified hydrogen atmosphere at a temperature of $T_{\text{gr}}=600\text{ }^\circ\text{C}$. An In-rich melt was prepared from undoped InAs and GaSb monocrystalline binary compounds with residual carrier concentrations $n=2\times 10^{16}\text{ cm}^{-3}$ and $p=1\times 10^{17}\text{ cm}^{-3}$, respectively. These constituents were dissolved into 7 N of In to make up the growth solution. The melt compositions and growth conditions (liquidus and supercooling temperatures) were obtained from thermodynamic calculation of the phase diagram for the $\text{Ga}_{0.84}\text{In}_{0.16}\text{As}_{0.22}\text{Sb}_{0.78}$ quaternary solid solution.

^{a)}Visiting research fellow at Lancaster University; electronic mail: mkd@iropt2.ioffe.rssi.ru

^{b)}Author to whom correspondence should be addressed; electronic mail: a.krier@lancaster.ac.uk

^{c)}Also with: A. F. Ioffe Physico-Technical Institute, St. Petersburg, Russia.

Photoluminescence (PL) measurements were carried out on the resulting epitaxial heterointerfaces with the sample in an Oxford Instruments continuous-flow liquid helium cryostat, which enabled temperature selection between 4 and 300 K. The photoluminescence was excited using the 488 nm line from an Ar ion laser. After passing through the sapphire window of the cryostat, the PL emission was focused into a Bentham 0.3 m monochromator using CaF₂ lenses and detected using a liquid N₂ cooled InSb photodiode and Stanford Research (SR850) digital phase-sensitive detector. A computer was used to control the monochromator and record the final signal using LABVIEW operating software.

RESULTS AND DISCUSSION

The Ga_{0.84}In_{0.16}As_{0.22}Sb_{0.78} layers obtained here had mirror-like surfaces and were of uniform thickness of about 0.8 μ m as observed by cross-sectional SEM. The layers were also examined using double crystal x-ray diffraction and found to be slightly lattice mismatched to the InAs substrate (280 ppm) at room temperature. The structures under investigation here were isotype single heterostructures since the Ga_{0.84}In_{0.16}As_{0.22}Sb_{0.78} layers were unintentionally doped and were *p* type with a residual hole concentration of $\sim 5 \times 10^{16}$ cm⁻³, whereas the *p*-type InAs substrate was deliberately compensated with Zn to a hole concentration of $p \sim 10^{17}$ cm⁻³. This was primarily to achieve high resistivity at 77 K and prevent parallel leakage as required for associated magnetotransport measurements. Hall measurements performed on standard "Hall cross" samples made from this material revealed the presence of a two-dimensional (2D) electron channel at the interface with a carrier concentration $n_e = 3 \times 10^{11}$ cm⁻² in single *p*-Ga_{0.84}In_{0.16}As_{0.22}Sb_{0.78}/*p*-InAs heterostructures at 4.2 K in low magnetic fields (<10 T). The electron Hall mobility was found to be as high as $\mu_H = 50\,000$ cm²/Vs at 77 K. More recently, Quantum Hall effect plateaus in a semimetal channel at the type II broken-gap *p*-Ga_{0.84}In_{0.16}As_{0.22}Sb_{0.78}/*p*-InAs heterointerface were observed.⁹

PL was observed from the samples at low temperature in the range $T = 5$ –35 K. The 5 K PL spectra for the samples under investigation contained three pronounced emission bands, one in the spectral range $h\nu = 0.56$ –0.68 eV and two further ones in the range $h\nu = 0.30$ –0.45 eV as shown in Fig. 1. The high-energy part of the PL spectrum corresponds to luminescence from the wide-gap Ga_{0.84}In_{0.16}As_{0.22}Sb_{0.78} solid solution, which has an energy gap of 0.644 eV.⁷ More precisely, the emission band has a peak at $h\nu_L = 0.622$ eV and can be associated with radiative transitions involving an acceptor level with an activation energy $E_{A1} = 22$ meV arising from a native lattice defect. This PL peak was observed to shift toward higher energies with increasing laser excitation as shown in Fig. 2. The "blueshift" of 6 meV and the asymmetric shape of the emission band with a high-energy tail is characteristic of Moss–Burstein filling at the bottom of the conduction band. The dependence of the emission band maximum and PL peak intensity on the excitation level was observed to be almost linear as shown in the inset of Fig. 2. In addition to the main PL emission band, a second much

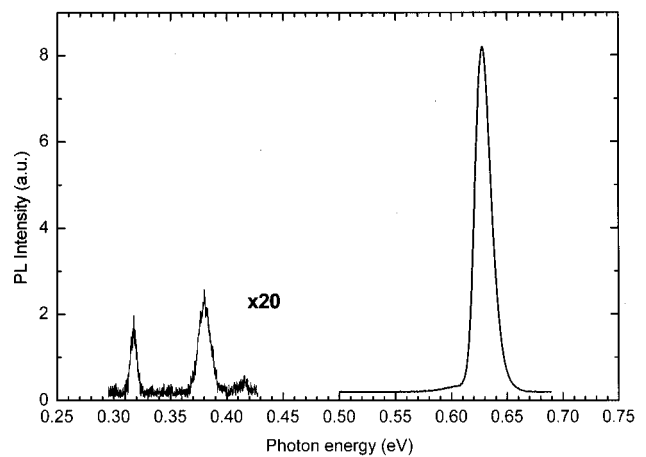


FIG. 1. A typical PL spectrum from the type II broken-gap single *P*-Ga_{0.84}In_{0.16}As_{0.22}Sb_{0.78}/*p*-InAs heterostructures measured at 5 K.

weaker emission band could also be deconvoluted from the spectrum, with a maximum at $h\nu_{DA} = 0.600$ eV. This emission band can be ascribed to radiative recombination involving a deep acceptor level with an activation energy of $E_{DA} = 44$ meV.⁷

The temperature dependence of the principle emission band ($h\nu_L = 0.622$ eV) associated with the bulk Ga_{0.84}In_{0.16}As_{0.22}Sb_{0.78} quaternary was also investigated and is shown in Fig. 3. However, the PL intensity rapidly quenched as the temperature increased from 20 to 35 K and only a small change in the spectral position of the PL peak with temperature was observed. The spectral position of the emission band maximum $h\nu_L = 0.621$ eV at $T = 35$ K is in good accordance with the temperature shift of the forbidden gap of the quaternary solid solution, since the energy gap becomes narrower by 3 meV with increasing temperature from 5 to 35 K.^{10,11}

The low-energy part ($h\nu = 0.30$ –0.45 eV) of the PL spectrum of Fig. 1 can be ascribed to radiative recombination originating from radiative transitions involving self-consistent quantum wells localized at the interface. The PL spectra in this spectral range exhibit two pronounced emission bands with peak photon energies at $h\nu_1 = 0.317$ eV and $h\nu_2 = 0.38$ eV, and with full width at half maximum (FWHM) of 5 and 12 meV, respectively (see Figs. 4 and 5). As shown in Fig. 4, the emission band $h\nu_2$ dominates the PL spectra at $T = 5$ K. Another emission band $h\nu_1$ appears at powers above 0.4 W. Then, further increasing the excitation results in a monotonous increase of the PL intensity for both emission bands until they both saturate at high pumping levels ($P > 4$ W) as shown in Fig. 6. In addition, a third high-energy emission band with peak energy $h\nu_3 = 0.416$ eV and FWHM = 10 meV was also observed at the highest excitation levels. This latter peak can be associated with band-to-band recombination in the bulk InAs substrate. The value of 0.416 eV is characteristic of interband transitions in InAs at low temperature and is in good agreement with observations obtained elsewhere.¹² The excitation dependence of the PL intensity at $T = 20$ K is slightly different in comparison to its behavior at 5 K (see Figs. 5 and 6). A redistribution of total

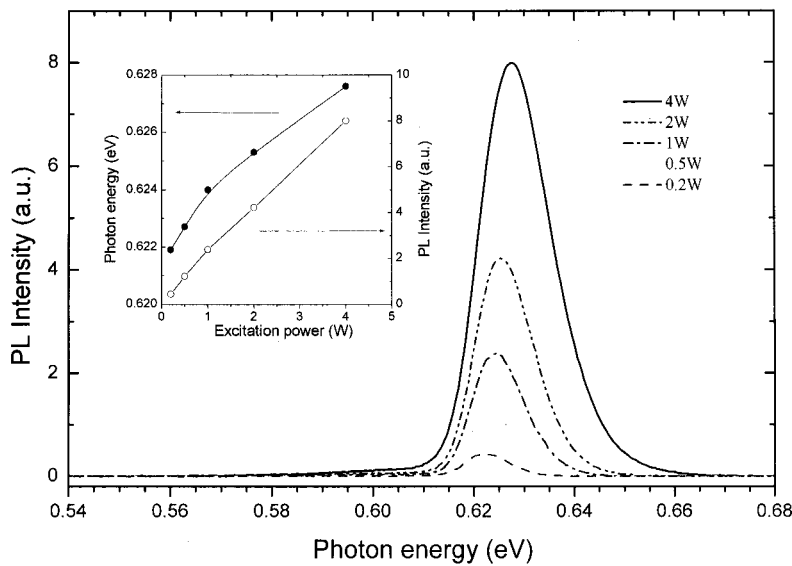


FIG. 2. PL spectra for undoped $\text{Ga}_{0.84}\text{In}_{0.16}\text{As}_{0.22}\text{Sb}_{0.78}$ solid solution at different pumping levels at 5 K. (Inset) The dependence of PL intensity and peak spectral position on laser excitation power.

intensity between $h\nu_1$ and $h\nu_2$ emission bands was observed. Furthermore, the excitation dependence of the PL intensity for the $h\nu_1$ emission band is linear, while the $h\nu_2$ emission band achieves a maximum and then decreases above 2 W.

A schematic energy diagram of band bending at the heterointerface and the possible radiative transitions is presented in Fig. 7. As shown in Fig. 7(a), when the heterojunction is formed, electrons from the $\text{Ga}_{0.84}\text{In}_{0.16}\text{As}_{0.22}\text{Sb}_{0.78}$ valence band flow into the empty InAs conduction band due to the crossing of the valence and conduction bands at the interface. A 2D electron gas is formed in the $\text{Ga}_{0.84}\text{In}_{0.16}\text{As}_{0.22}\text{Sb}_{0.78}/\text{InAs}$ heterojunction within the quantum well on the InAs side, and an equivalent number of holes that are left behind reside near the heterointerface on the $\text{Ga}_{0.84}\text{In}_{0.16}\text{As}_{0.22}\text{Sb}_{0.78}$ side, resulting in the formation of a triangular potential well. The strong intrinsic electric field produced at the interface holds the electrons and holes to-

gether in self-consistent quantum wells and determines the carrier population density in the semimetal channel maintained by the common bulk Fermi level E_F of the heterojunction at thermodynamic equilibrium.

Under optical excitation, the photogenerated carriers fill the quantum wells at both sides of the interface, such results in increased band bending in the vicinity of the heterointerface [Fig. 7(b)]. We assume the $h\nu_1$ emission band observed in the experiment can be ascribed directly to radiative tran-

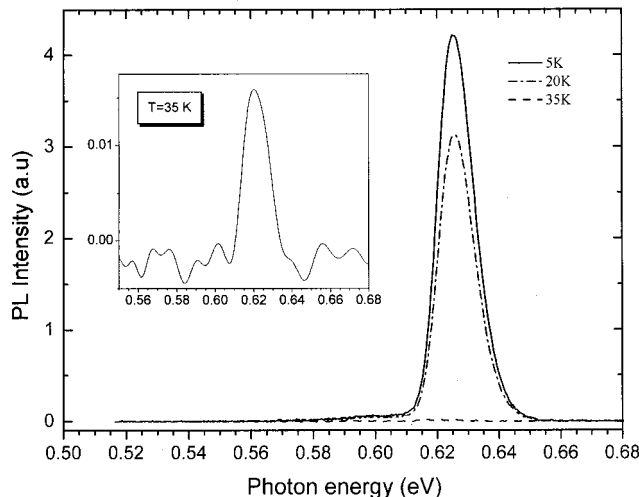


FIG. 3. PL spectra for undoped $\text{Ga}_{0.84}\text{In}_{0.16}\text{As}_{0.22}\text{Sb}_{0.78}$ solid solution at the same pumping level at different temperatures. (Inset) The magnification of the PL spectrum at 35 K.

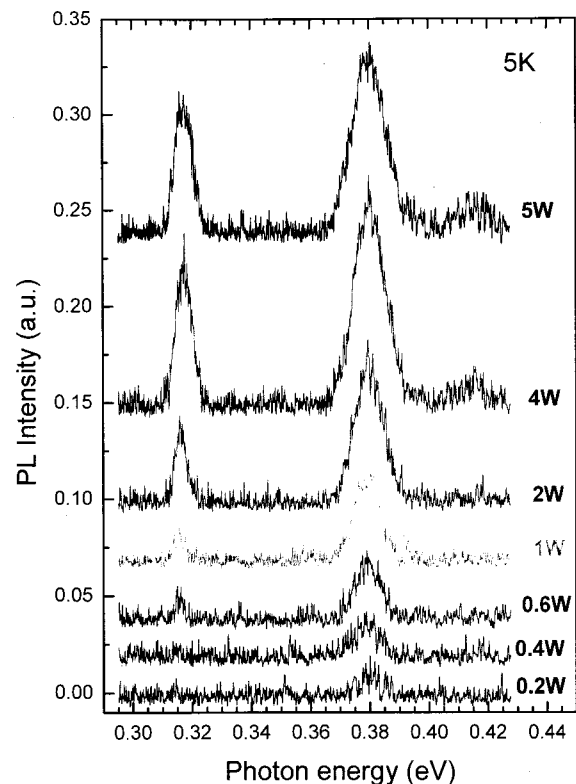


FIG. 4. The low-energy part of the PL spectra for the type II broken-gap $\text{P-Ga}_{0.84}\text{In}_{0.16}\text{As}_{0.22}\text{Sb}_{0.78}/p\text{-InAs}$ heterostructure at different pumping levels measured at 5 K.

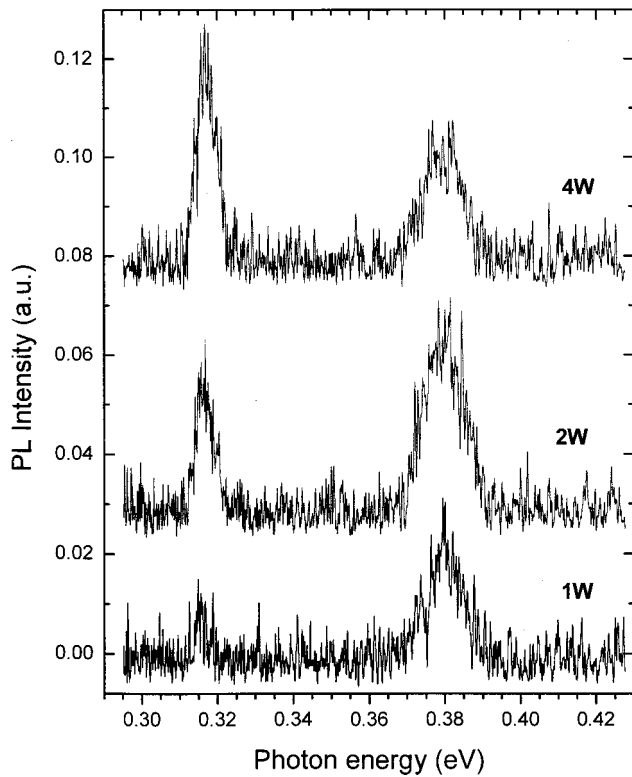


FIG. 5. The low-energy part of the PL spectra for the type II broken-gap $P\text{-Ga}_{0.84}\text{In}_{0.16}\text{As}_{0.22}\text{Sb}_{0.78}/p\text{-InAs}$ heterostructure at different pumping levels measured at 20 K.

sitions between electron and hole quantum well subbands in the semimetal channel at the $P\text{-Ga}_{0.84}\text{In}_{0.16}\text{As}_{0.22}\text{Sb}_{0.78}/p\text{-InAs}$ interface. At low pumping levels, the potential barrier for holes ($\Delta E_V \sim 0.48$ eV) formed by the valence band discontinuity at the interface prevents their penetration into the InAs valence band, whereas there is no limit to the movement of electrons into the InAs conduction band. In the case of the $h\nu_2$ emission band, electrons from the conduction band of the InAs recombine with holes localized in the deep acceptor states of the InAs. Due to the heavy compensation of donor levels by shallow Zn acceptors in the InAs sub-

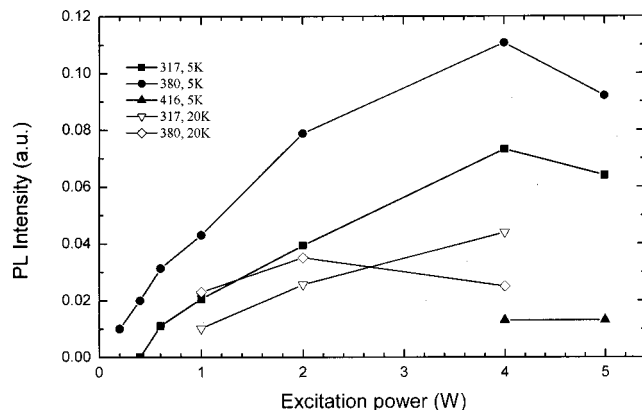


FIG. 6. Dependence of the PL intensity on the excitation power for $h\nu_1$ (317 meV), $h\nu_2$ (380 meV), and $h\nu_3$ (416 meV) emission bands at 5 and 20 K.

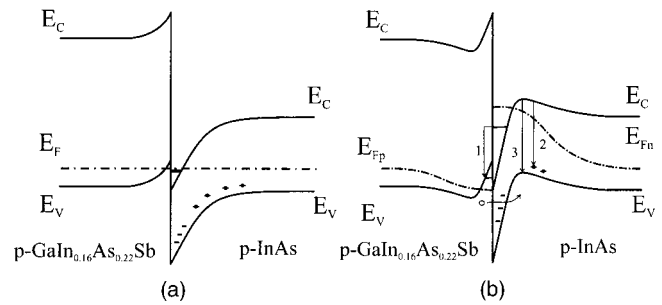


FIG. 7. A schematic energy diagram of the type II broken-gap $P\text{-Ga}_{0.84}\text{In}_{0.16}\text{As}_{0.22}\text{Sb}_{0.78}/p\text{-InAs}$ heterostructure: (a) at thermodynamic equilibrium and (b) under optical excitation conditions. The arrows indicate possible radiative transitions.

strate, radiative recombination involving the deep acceptor states becomes possible, and therefore the $h\nu_2$ emission band can be observed.

Further raising the pumping level increases the concentration of electrons and holes constrained by the intrinsic electric field of the heterojunction. The increasing carrier accumulation in the semimetal channel results in the quantum wells becoming deeper, and therefore electron and hole subbands in the quantum wells can be easily formed. Thus, radiative recombination can arise from transitions between subbands localized on opposite sides of the heterointerface. The small blueshift of the $h\nu_1$ emission band maximum, of about 3 meV, with increasing excitation power is in good accordance with the increasing energy separation between these subbands, while the $h\nu_2$ peak remains at constant energy.

At high excitation, the width of the potential barrier for holes becomes sufficiently thin, so that hole tunneling from the quantum well on the $\text{Ga}_{0.84}\text{In}_{0.16}\text{As}_{0.22}\text{Sb}_{0.78}$ side through the barrier into the valence band of the InAs takes place. These holes accumulate at the top of the valence band in the shallow potential well adjacent to the electron channel. Consequently, conduction band–valence band recombination in the InAs [$h\nu_3$ –transition 3 in Fig. 7(b)] becomes possible, which in turn leads to quenching of the PL intensity of both the $h\nu_1$ and $h\nu_2$ emission bands (see Fig. 6).

CONCLUSIONS

Low temperature photoluminescence has been observed from $\text{Ga}_{0.84}\text{In}_{0.16}\text{As}_{0.22}\text{Sb}_{0.78}/\text{InAs}$ single heterojunctions grown by LPE. The spectra exhibit three pronounced emission bands in the spectral region from 0.30 to 0.68 eV. The low-energy part of the PL spectrum can be associated with interface-induced radiative transitions involving a semimetal channel produced at the P – p isotype heterointerface. The emission band with a peak photon energy at $h\nu_1 = 0.317$ eV and $\text{FWHM} = 5$ meV can be ascribed to radiative transitions between electron and hole quantum well subbands localized on opposite sides of the interface. The emission band with a maximum at $h\nu_2 = 0.380$ eV results from radiative transitions involving the deep acceptor states in the bulk of the InAs substrate. The remaining features in the spectra are associated with recombination in the quaternary layer ($h\nu_L = 0.622$ eV) and in the InAs substrate ($h\nu_3 = 0.416$ eV).

ACKNOWLEDGMENTS

The authors would like to thank Dr. E. Hulicius and Dr. P. Svoboda from The Institute of Physics, Prague, Czech Republic, for carrying out the related Hall measurements. The authors also wish to thank EPSRC for providing a visiting research fellowship for Dr. K. Moiseev.

¹G. W. Charache *et al.*, J. Appl. Phys. **85**, 2247 (1999).

²M. P. Mikhailova, K. D. Moiseev, O. G. Ershov, and Yu. P. Yakovlev, Semiconductors **30**, 223 (1996).

³T. I. Voronina, T. S. Lagunova, M. P. Mikhailova, K. D. Moiseev, A. E. Rozov, and Yu. P. Yakovlev, Semiconductors **34**, 189 (2000).

⁴G. G. Zegrya, M. P. Mikhailova, T. N. Danilova, A. N. Imenkov, K. D. Moiseev, V. V. Sherstnev, and Yu. P. Yakovlev, Semiconductors **33**, 97 (1999).

⁵K. D. Moiseev, M. P. Mikhailova, O. G. Ershov, and Yu. P. Yakovlev, Phys. Tech. Lett. **23**, 151 (1997).

⁶K. D. Moiseev, A. A. Toropov, Ya. V. Terentiev, M. P. Mikhailova, and Yu. P. Yakovlev, Semiconductors **34**, 1376 (2000).

⁷K. D. Moiseev, M. P. Mikhailova, Yu. P. Yakovlev, T. Šimeček, E. Hulicius, and J. Oswald, J. Appl. Phys. (to be published).

⁸M. P. Mikhailova, K. D. Moiseev, R. V. Parfeniev, N. L. Bazhenov, V. A. Smirnov, and Yu. P. Yakovlev, IEE Proc.: Optoelectron. **145**, 268 (1998).

⁹K. D. Moiseev, V. A. Berezovets, M. P. Mikhailova, V. I. Nizhankovskii, R. V. Parfeniev, and Yu. P. Yakovlev, Surf. Sci. **482–485**, 1083 (2002).

¹⁰K. D. Moiseev, M. P. Mikhailova, Yu. P. Yakovlev, T. Šimeček, E. Hulicius, and J. Oswald, J. Electron. Mater. (to be published).

¹¹K. D. Moiseev, A. Krier, and Yu. P. Yakovlev, J. Electron. Mater. (to be published).

¹²Y. Lacroix, C. A. Tran, S. P. Watkins, and M. L. W. Thewalt, J. Appl. Phys. **80**, 6416 (1996).